A Miniaturized Dual-Band Implantable Antenna with Improved Impedance Matching via Shorting Vias and CSRRs

Herman Yuliandoko
Department of Electrical Engineering, Institut Teknologi Sepuluh Nopember, Surabaya, Indonesia
herman.yuliandoko@poliwangi.ac.id

Puji Handayani
Department of Electrical Engineering, Institut Teknologi Sepuluh Nopember, Surabaya, Indonesia
puji@ee.its.ac.id

Eko Setijadi
Department of Electrical Engineering, Institut Teknologi Sepuluh Nopember, Surabaya, Indonesia
ekoset@ee.its.ac.id (corresponding author)

Received: 30 September 2025 | Revised: 17 November 2025 | Accepted: 25 November 2025

 DOI: https://doi.org/10.48084/etasr.15238

ABSTRACT

Implantable antennas represent a significant advancement in wireless technology for medical applications, supporting Implantable Medical Devices (IMDs) with various essential functions. To meet the stringent requirements of IMDs, such as compact size, biocompatibility, and structural integrity, implantable antennas must be optimized accordingly. This research addresses these challenges by employing the Defected Ground Structure (DGS) miniaturization technique, combined with the integration of Complementary Split Ring Resonators (CSRRs) in a dual-band antenna design, to achieve a small, multifunctional antenna. The proposed antenna operates within the frequency bands of 2.4–2.48 GHz for Wireless Power Transfer (WPT) and 1.395–1.4 GHz for Wireless Medical Telemetry Service (WMTS). Impedance matching is critical for optimal antenna performance, which is facilitated in this study by the use of shorting vias. These vias not only aid in achieving impedance matching but also contribute to the miniaturization process. The resulting antenna, with dimensions of 9.3 mm × 8.75 mm × 0.635 mm, demonstrates a size reduction of up to 90% through CSRR-based miniaturization. Furthermore, the application of shorting vias has proven effective in improving impedance matching, resulting in a return loss value within the acceptable range despite the dual-frequency operation.

Keywords-miniaturization; dual-band; implantable antenna; Complementary Split Ring Resonator (CSRR)

I. INTRODUCTION

Wireless technology has seen remarkable growth, driven by its flexibility and wide application across various aspects of human life [1]. One application of wireless technology is Implantable Medical Devices (IMDs), which include an antenna that plays a crucial role as a receiver or transmitter. IMDs have transformed healthcare by enabling patient monitoring, facilitating communication with external devices, and supporting wireless charging [2]. However, these innovations present challenges in designing implantable antennas that are compact, efficient, and adhere to high-quality standards.

The application of antennas in technologies such as Magnetic Resonance Imaging (MRI), Radio-Frequency Identification (RFID)-based patient monitoring, and hyperthermia therapy for cancer treatment highlights their crucial role in enhancing the efficiency and effectiveness of healthcare services [3]. For patients with heart disease, cardiac pacemakers are used to monitor and support proper heart function, implantable glucose monitors track blood sugar levels, and neurostimulators stimulate brain nerves to aid in the treatment of Parkinson's disease [4]. In addition to serving as a communication medium, the antenna also facilitates Wireless Power Transfer (WPT), transmitting energy from external sources to the implantable device, thereby charging the battery within the IMD [5]. Implantable antennas must possess compact characteristics, being small, flexible, and capable of performing effectively in their applications [6].

One fundamental design consideration for implantable antennas is size minimization. However, reducing the antenna's physical dimensions often leads to a degradation in

electromagnetic performance, including impedance matching, gain, and bandwidth. Consequently, antenna miniaturization techniques play a vital role in optimizing a compact design while maintaining acceptable performance levels. Previous studies have explored antenna miniaturization by combining fractal and Defected Ground Structure (DGS) techniques at both single and dual frequencies [5, 7]. Miniaturization at dual frequencies introduces unique difficulties, as it requires not only reduced antenna dimensions but also the preservation of the target frequency. Consequently, the application of miniaturization techniques and their respective stages is crucial for achieving small antenna sizes, which significantly influence the overall miniaturization process.

In [8], a dual-band meander line antenna was designed for WPT and Wireless Medical Telemetry Service (WMTS). In addition, shorting pins were used to produce an antenna size of 11 mm × 11 mm × 1.28 mm. A dual-band meander line antenna was also used in [9], resulting in an antenna size of 10 mm × 10 mm × 0.635 mm. Slot technology was used in [10], but it was still single-frequency, whereas authors in [11] used dual-band frequencies, although the size was still very large. Patch antennas are employed in single low-frequency Medical Implantable Communication Service (MICS) applications and have been simulated with varying substrate thicknesses [12]. While dual-band antennas for high frequency applications have been studied in [13], the antenna size remains significantly large. Beyond size reduction, other critical parameters, such as performance, limited battery lifetime, and patient safety, present additional challenges for researchers [14, 15]. Some studies propose WPT as a solution to address the issue of limited battery lifetime in IMDs [16, 17].

IMD frequency operational standards have been set by the International Telecommunication Union (ITU), which categorizes them into several frequency bands. These include the MICS with a bandwidth of 402–405 MHz, and the WMTS operating in the 1.395–1.400 GHz and 1.427–1.432 GHz ranges [18]. Additionally, WPT frequencies are regulated by the Industrial, Scientific, and Medical (ISM) bands, which cover 433–434 MHz, 902–908 MHz, 2.4–2.48 GHz, and 5.715–5.875 GHz [4].

Various feeding techniques are employed in microstrip antennas, including the line feeding, coaxial feeding (or probe feeding), aperture-coupled feeding, and proximity-coupled feeding techniques [19, 20]. Most miniaturization efforts focus on single-frequency antennas, but multi-frequency antennas offer the advantage of using one antenna for many functions, although multi-band antennas are more difficult to design and fabricate.

This research introduces a novel approach by combining miniaturization techniques that incorporate high permittivity substrates, Complementary Split Ring Resonator (CSRR) techniques as a DGS, and shorting vias for impedance matching. The use of high permittivity substrates has been shown to reduce antenna size, although it can negatively impact bandwidth [21]. However, high permittivity also increases sensitivity, which presents challenges in antenna design, particularly when using simulation tools like CST. Line-feed techniques are rarely used in antenna miniaturization because feedline dimensions can increase the overall size of the antenna. Despite this, line-feed design and implementation are simpler compared to other feeding methods. Additionally, this study incorporates dual frequencies of 1.395 GHz for telemetry and 2.4 GHz for WPT, which significantly increases the complexity of miniaturizing the antenna.

II. ANTENNA DESIGN

This study was conducted in several stages, beginning with the design of a 2.4 GHz antenna for WPT. In this phase, an equivalency analysis was also performed using Advanced Design System (ADS). The second stage involved evaluating the effectiveness of shorting vias as a method for impedance matching. Subsequently, a dual-band antenna design was developed, operating at 1.3 GHz and 2.4 GHz, with the 1.3 GHz frequency allocated for WMTS. The final stage focused on the miniaturization process, employing DGS with CSRR.

The antenna utilized in this study, shown in Figure 1, is a rectangular microstrip antenna, which is commonly employed by researchers due to its advantages, such as ease of design, flexibility, and low cost. The following are some of the commonly used formulas in the design process [22, 23]:

$$wp = \frac{c}{2f_r}\sqrt{\frac{2}{\varepsilon_r+1}} \quad (1)$$

$$\varepsilon_{r,eff} = \left(\frac{\varepsilon_r+1}{2}\right) + \left(\frac{\varepsilon_r-1}{2}\right)\left(1+12\frac{h}{wp}\right)^{-\frac{1}{2}} \quad (2)$$

$$\Delta l = \frac{0.412h\left(\varepsilon_{r,eff}-0.8\right)\left(\frac{wp}{h}+0.264\right)}{\left(\varepsilon_{r,eff}-0.258\right)\left(\frac{wp}{h}-0.8\right)} \quad (3)$$

$$lp = \frac{c}{2f_r\sqrt{\varepsilon_{r,eff}}} - 2\Delta l \quad (4)$$

$$wg = wp + 6h \quad (5)$$

$$lg = lp + 6h \quad (6)$$

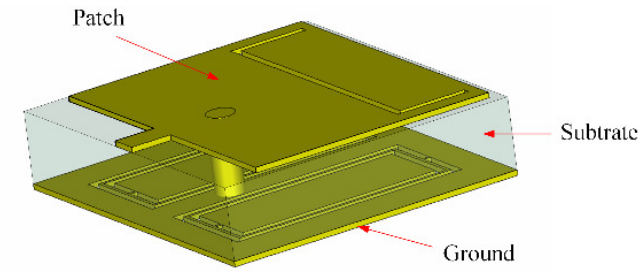

Fig. 1. Rectangular microstrip antenna design.

For all parameters in (1)–(6), Δl denotes the length extension resulting from the fringing field effect on one side of the patch, whereas the definitions of the remaining parameters are provided in Table I. We propose an antenna design, as shown in Figure 2, that incorporates shorting vias for impedance matching and CSRRs in the grounding system. The placement of the shorting vias is crucial, as it can cause a shift from the target frequency. Additionally, the diameter of the shorting vias is determined based on established references, with the pin diameter (D) ranging from 0.1 to 0.5 mm [24].

TABLE I. ANTENNA DIMENSIONS

No	Antenna parameter	Symbol	Dimensions
1	Frequency	f_r	2.45 GHz
2	Dielectric constant	ε_r	10.2
3	Substrate thickness	h	0.635 mm
4	Effective dielectric constant	$\varepsilon_{r,eff}$	9.64
5	Patch width	wp	28 mm
6	Patch length	lp	20 mm
7	Ground plane width	wg	29 mm
8	Ground plane length	lg	30 mm
9	Line feed width	wf	0.8 mm
10	Line feed length	lf	9.6 mm
11	Diameter of shorting vias	D	0.5 mm
12	Pin position	W	1.6 mm

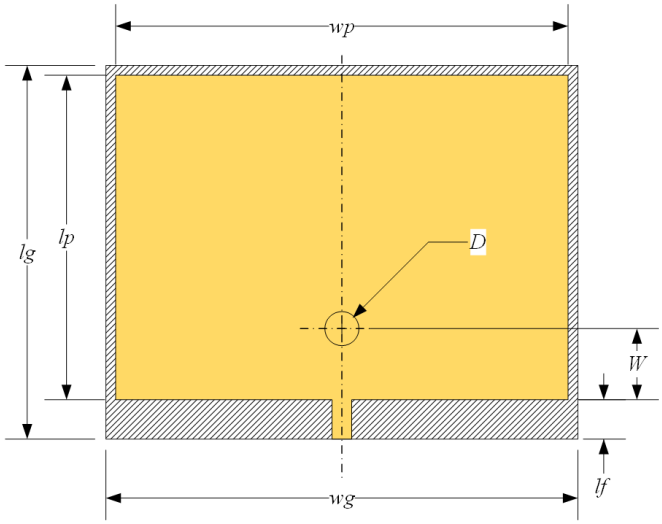

Fig. 2. Rectangular microstrip antenna with shorting vias.

III. RESULTS

The dimensions of the antenna are derived using (1)–(6), with Duroid Roger 3010 selected as the substrate material and copper as the patch material, having a thickness of 0.035 mm. The choice of substrate is driven by its high dielectric constant, which facilitates the miniaturization of the antenna. Furthermore, the thin substrate thickness enhances its suitability for applications in implantable antennas.

The shorting vias are represented as transmission line segments whose lengths correspond to the thickness of the microstrip antenna. This modeling approach results in an equivalent circuit, as shown in Figure 3, characterized by inductive (L) and capacitive (C) elements, which are systematically incorporated in both series and parallel configurations to accurately capture the antenna's electromagnetic behavior [25]. Changes in the resistance, inductance, and capacitance values in the equivalent circuit have a significant impact on the S_{11} bandwidth.

Figure 4 illustrates that variations in capacitance and inductance values lead to changes in frequency, whereas alterations in resistance values result in modifications to the return loss. Specifically, variations in capacitance and inductance result in a shift in the frequency value, whereas changes in resistance lead to modifications in the return loss.

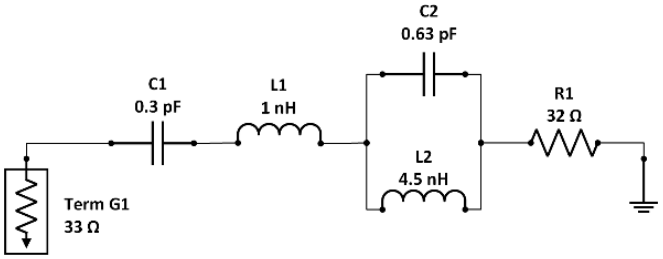

Fig. 3. Equivalent circuit of rectangular microstrip antenna with shorting vias.

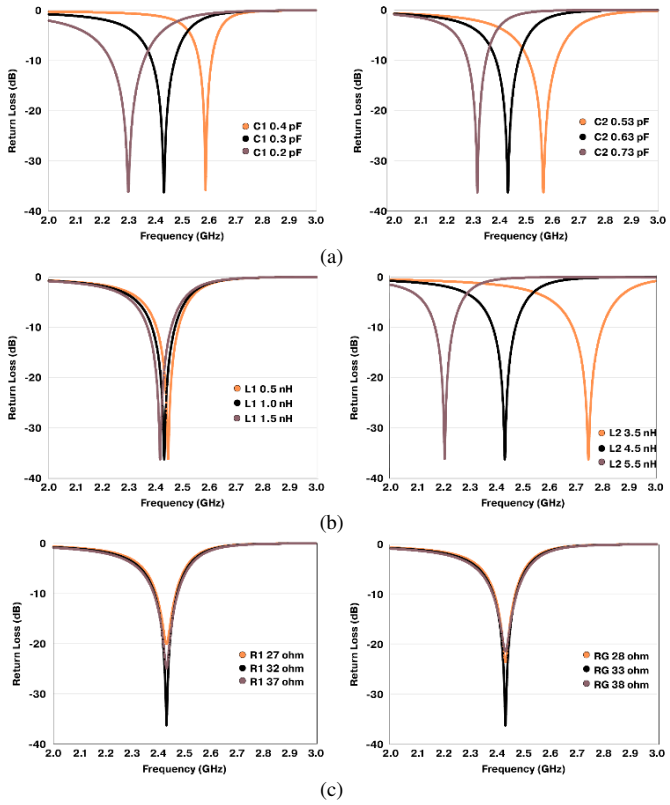

Fig. 4. Effect of equivalent circuit components on S_{11}: (a) capacitances C1 & C2, (b) inductances L1 & L2, (c) resistances R1 & RG.

The antenna simulation results using CST and the equivalent circuit in ADS were compared. The findings revealed that both simulations exhibited similar outcomes, with a return loss of –36.243 dB at 2.431 GHz in the ADS simulator and –36.254 dB at 2.443 GHz in CST, as depicted in Figure 5.

Shorting vias, depicted in Figure 6, are employed as an impedance matching method. They electrically connect the patch to the ground plane, effectively increasing the radiated area without physically enlarging the antenna, which enhances gain at resonance [25]. A parametric analysis was performed by varying the position of the shorting vias or pin position (W) to investigate its influence on the resonant frequency and reflection coefficient. The W parameter was adjusted along the Y-axis (vertical direction) from 0 to 10 mm (see Figure 2).

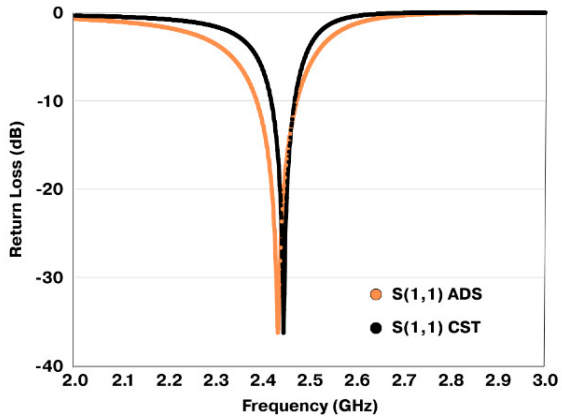

Fig. 5. S_{11} of the 2.4 GHz antenna using CST and ADS.

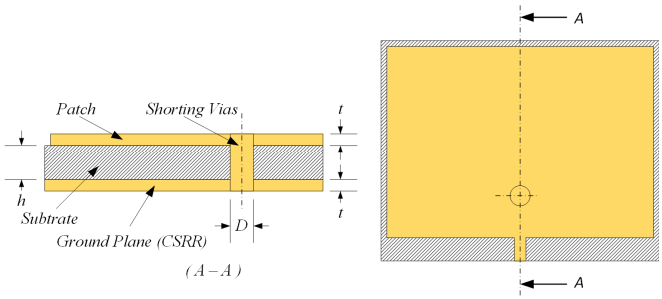

Fig. 6. Side view (A-A) of the rectangular microstrip antenna showing the shorting vias.

As illustrated in Figure 7, variations in W have a substantial impact on the reflection coefficient, highlighting the critical sensitivity of the antenna performance to the placement of the shorting vias. The reflection coefficient value ranges from -1 to 1. An antenna is considered to have good impedance matching if its reflection coefficient value is close to 0, which indicates that almost all of the incoming power is received by the antenna without being reflected back. Conversely, a value closer to 1 or -1 indicates a significant impedance mismatch, where most of the power is reflected back. Variations in the W parameter significantly affect the reflection coefficient. As the W value increases, the reflection coefficient also increases, indicating a deterioration in impedance matching. In this study, the optimal reflection coefficient was observed at W = 1.6 mm (pin position), corresponding to a frequency of 2.438 GHz with a reflection coefficient of 0.025 dB. The reflection coefficient represents the ratio between the load impedance and the characteristic impedance of the transmission line, as defined in the following equation [26]:

$$\gamma = \frac{Z_{in} - Z_0}{Z_{in} + Z_0} \quad (7)$$

where:

- γ denotes the reflection coefficient.
- Z_{in} denotes the input impedance.
- Z_0 denotes the characteristic impedance.

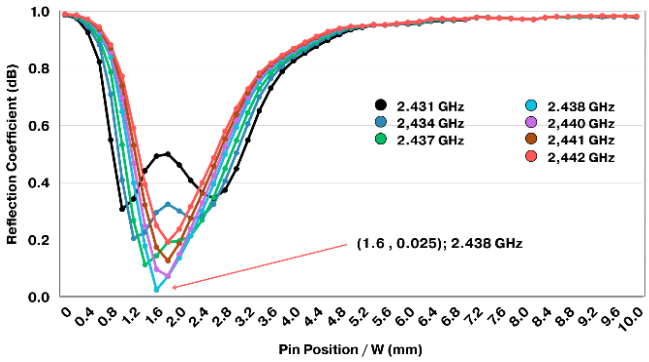

Fig. 7. Effect of shorting vias position (W) on the reflection coefficient of the antenna.

Figures 8 and 9 illustrate that the impedance of the 2.4 GHz antenna closely approximates the ideal value of 50 Ω, thereby validating the effectiveness of the impedance matching improvement achieved using the shorting vias technique. As previously mentioned, this research presents a dual-band antenna, and additional steps are required to achieve the second frequency range of 1.395–1.400 GHz for WMTS. The slot technique is employed in this study, as it has been demonstrated to be effective in creating multi-band frequencies [27]. Additionally, the slot technique has been utilized in the miniaturization of multiband antennas, as reported in [11].

The U-slot in Figure 10 is designed to generate two resonant frequencies with the following dimensions: *x1* = 3.7 mm, *x2* = 3.7 mm, *y1* = 3.5 mm, and *y2* = 0.6 mm, whereas the slot dimensions *b1* and *b2* are 0.5 mm. These parameters significantly influence the resulting frequencies, particularly the values of *x1* and *x2*. Additionally, the dimensions *y1* and *y2* affect the return loss magnitude. Simulation results using CST show that the first frequency is at 1.398 GHz with a return loss of –12.650 dB, whereas the second frequency is at 2.486 GHz with a return loss of –22.836 dB.

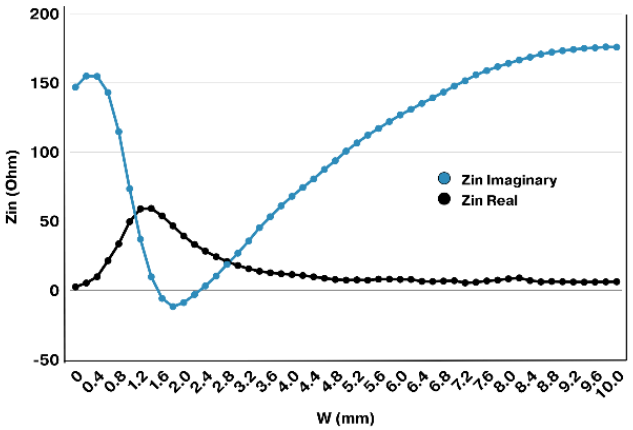

Fig. 8. Real and imaginary components of the reflection coefficient.

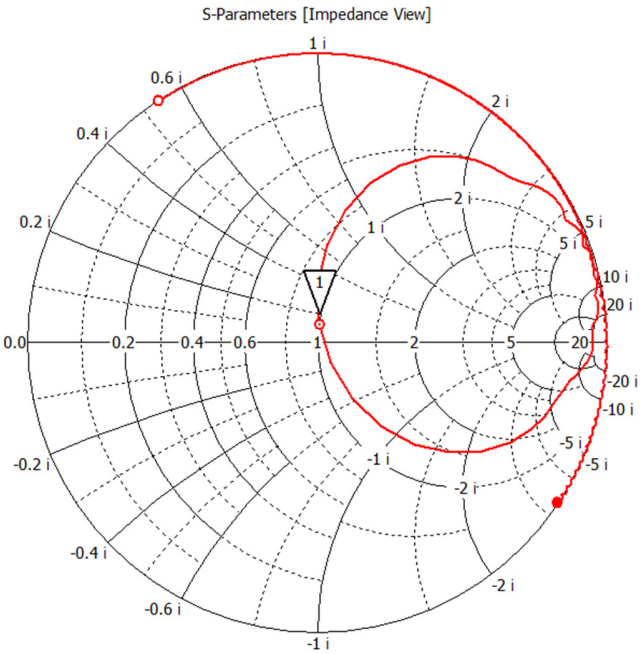

Fig. 9. Impedance matching at 2.4 GHz shown on the Smith chart.

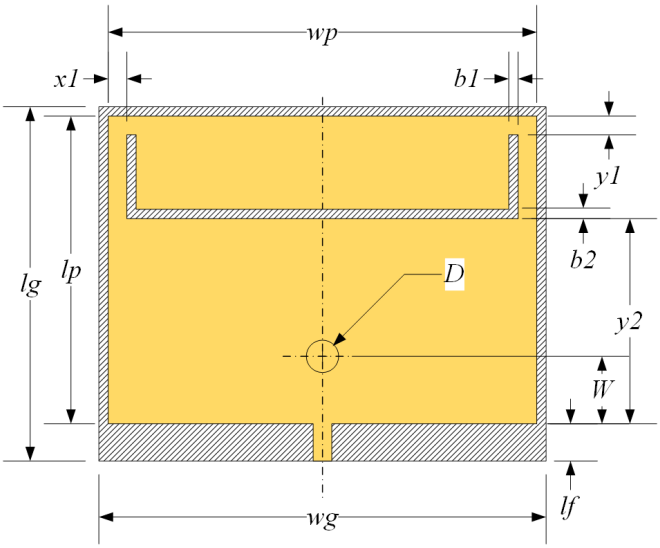

Fig. 10. U-slot patch structure.

Additionally, an analysis was conducted using ADS to derive the equivalent circuit of the U-slot patch antenna, as referenced in the literature. This circuit was subsequently integrated with the equivalent circuit shown in Figure 3, with the combined model illustrated in Figure 11 [28].

The capacitance and inductance values in the equivalent circuit have a significant impact on the frequency shift, whereas the resistance predominantly affects the return loss. The resulting S_{11} response from the simulations is shown in Figure 12, which compares the CST antenna results with those from the ADS equivalent circuit. As illustrated, the CST simulation and the U-slot equivalent circuit produce closely matching results, although the ADS response exhibits a slightly wider bandwidth than CST.

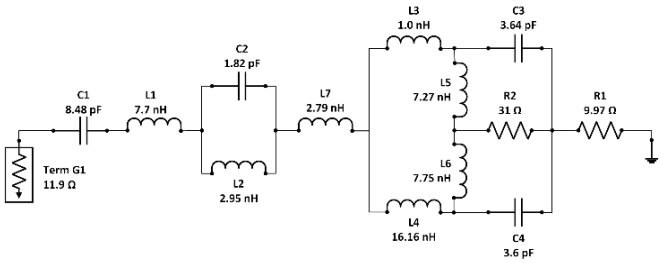

Fig. 11. Equivalent circuit diagram of the antenna with U-slot integration.

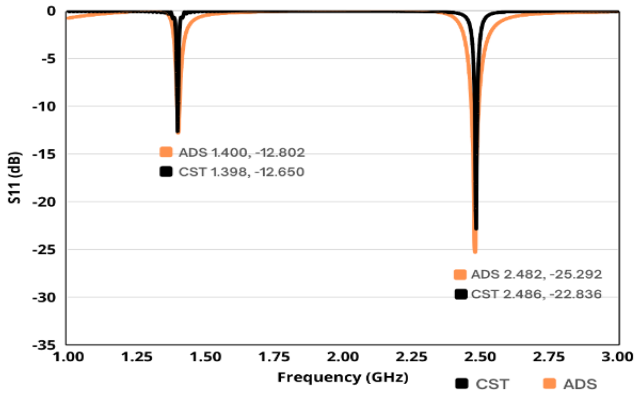

Fig. 12. S_{11} of the antenna with U-slot patch using CST and ADS.

This study also incorporates a CSRR placed on the ground plane to support the miniaturization of the antenna. The CSRR is a well-established metamaterial structure commonly employed in antenna design to achieve miniaturization without compromising radiation performance. As a variation of the Split Ring Resonator (SRR), CSRR utilizes resonance to modulate the electromagnetic field distribution around the antenna [29].

In this microstrip antenna design, the CSRR is positioned on the ground plane to modify the impedance properties and reduce the overall size of the antenna, as illustrated in Figure 13. The detailed CSRR parameter values used in the design are provided in Table II.

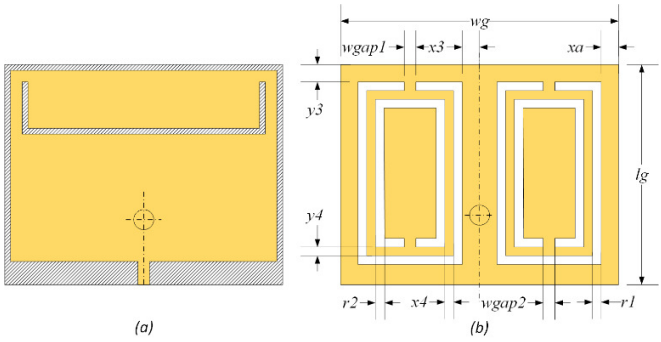

Fig. 13. (a) Microstrip patch, (b) CSRR-based DGS on the ground plane.

TABLE II. CSRR DIMENSIONS

Parameter	Dimension (mm)	Parameter	Dimension (mm)
x1	0.5	*y4*	0.1
b1	0.1	*wgap1*	0.1
y1	4.7	*x5*	0.3
y2	0.4	*r2*	0.2
b2	0.1	*y5*	0.3
x2	0.5	*x6*	0.3
x3	0.5	*y6*	0.3
y3	0.6	*wgap2*	0.1
r1	0.2	*xa*	1.4
x4	0.1		

The surface current distribution in Figure 14 indicates that the current is predominantly concentrated around the slot or CSRR region. This concentrated current path is desirable, as it enhances effective radiation by intensifying the electromagnetic activity within the resonant structure.

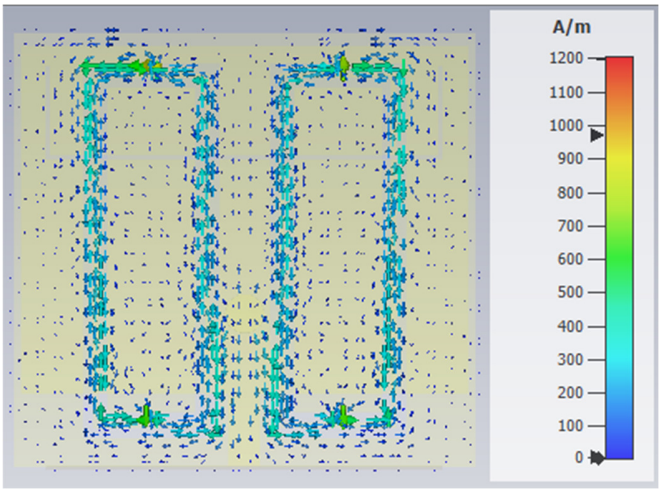

(a)

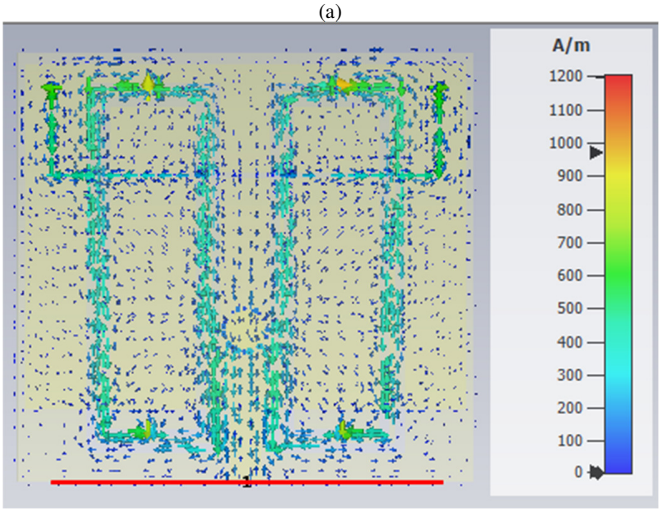

(b)

Fig. 14. Surface current distribution: (a) CSRR on the ground plane, (b) patch surface.

Figure 15 presents the simulated S_{11} response of the antenna after incorporating the CSRR structure into the ground plane. The CSRR is introduced to achieve antenna miniaturization while preserving impedance characteristics and overall performance. The results indicate that, although the antenna dimensions are reduced, the S_{11} response remains largely consistent with that of the original design.

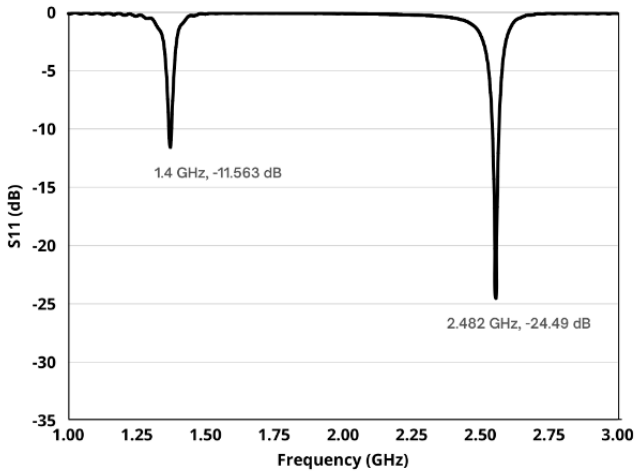

Fig. 15. S_{11} of the antenna with CSRR-based DGS.

Table III indicates that incorporating a CSRR-based DGS reduces the antenna dimensions from 29 mm × 30 mm in the original design to 9.3 mm × 8.75 mm after miniaturization, corresponding to a size reduction of approximately 90%. These results validate the effectiveness of the proposed miniaturization technique. Moreover, the return loss parameter (S11) meets the target specification despite a modest reduction in realized gain compared with the baseline.

TABLE III. ANTENNA MINIATURIZATION

No	Antenna parameter	Original (mm)	With U-slot (mm)	With CSRR DGS (mm)
1	*wg*	29	28.5	9.3
2	*lg*	30	30	8.75
3	*wp*	28	28	9
4	*lf*	9.6	7.5	1.5
5	*lp*	20	20	7
6	*wf*	0.8	0.6	0.65
7	*w*	1.6	2.4	1.6
8	*D*	0.5	0.5	0.4

The radiation pattern in Figure 16 exhibits a predominantly unidirectional profile with a focused main lobe, although the magnitude remains relatively low. This behavior is typical of miniaturized implantable antennas, which inherently experience reduced gain due to their compact size. Nevertheless, previous studies have shown that the integration of metamaterial structures can improve gain performance by enhancing radiation efficiency. Table IV compares the proposed antenna with previously reported implantable antenna designs, highlighting improvements in size, S11 levels, and bandwidth.

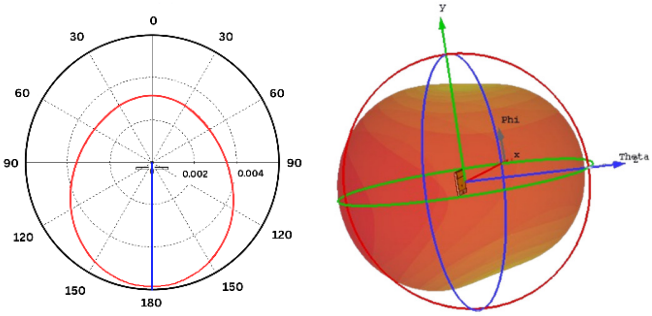

Fig. 16. Radiation pattern of the miniaturized implantable antenna.

TABLE IV. COMPARISON OF MINIATURIZED ANTENNA DESIGNS

Ref	Antenna size (mm)	Antenna type	Frequency	S_{11} (dB)	Bandwidth (MHz)
[8]	11 × 11 × 1.28	Meander line	Dual, 1.46 GHz; 2.42 GHz	–25.78; –39.95	45; 60.7
[9]	10 × 10 × 0.635	Meander line	Dual, 1.4 GHz; 2.4 GHz	–25; –34	3.57; 6.37
[13]	37 × 35 × 1.6	Circular patch	Dual, 3.7 GHz; 6.2 GHz	–30; –32	–
[12]	14 × 12 × 1.27	Rectangular	Single, 404 MHz	–32.58	26
[10]	10 × 10 × 1.27	Slot patch	Single, 2.45 GHz	–31	16.3
This work	9.3 × 8.75 × 0.7	Rectangular	Dual, 1.4 GHz; 2.48 GHz	–11.56; –24.49	12.1; 27.6

IV. CONCLUSION

This research shows that the use of shorting vias can effectively optimize impedance matching, whereas miniaturization techniques incorporating Complementary Split Ring Resonators (CSRRs) can reduce antenna dimensions by up to 90% compared with those of conventional designs. In addition, the development of dual-band implantable antennas for Wireless Power Transfer (WPT) and Wireless Medical Telemetry Service (WMTS) presents significant challenges in antenna design and impedance matching. Nevertheless, dual-band operation offers considerable advantages for Implantable Medical Device (IMD) applications. Fabricating antennas at very small sizes remains challenging and requires high-precision equipment, highlighting opportunities for further research into fabrication capabilities or the use of metamaterials to enhance antenna performance. Additionally, the equivalent circuit analysis shows that variations in resistance mainly affect the return loss, whereas changes in capacitance and inductance primarily affect the antenna bandwidth.

ACKNOWLEDGMENT

The researcher wishes to express gratitude to the members of the Jaringan Telekomunikasi Laboratory for their valuable support throughout this research. Additionally, sincere appreciation is extended to the Ministry of Education, Culture, Research, and Technology, the Center for Higher Education Funding and Assessment (PPAPT), and the Indonesian Endowment Fund for Education (LPDP) for their financial assistance through the BPI (Beasiswa Pendidikan Indonesia) scholarship, as stated in SK NOMOR 00773/J5.2.3./BPI.06/9/2022, which made this research possible.

REFERENCES

[1] N. A. M. Nasir, H. Ja'afar, H. Baba, and N. H. A. Aziz, "A Study on Different Slot Position for Designing Dual Band Microstrip Antenna for 5G Wireless Communication," *IOP Conference Series: Materials Science and Engineering*, vol. 1176, no. 1, Aug. 2021, Art. no. 012014, https://doi.org/10.1088/1757-899X/1176/1/012014.

[2] M. El Atrash, M. A. Abdalla, and H. M. Elhennawy, "A Wearable Dual-Band Low Profile High Gain Low SAR Antenna AMC-Backed for WBAN Applications," *IEEE Transactions on Antennas and Propagation*, vol. 67, no. 10, pp. 6378–6388, Oct. 2019, https://doi.org/10.1109/TAP.2019.2923058.

[3] A. Gupta, A. Kansal, and P. Chawla, "A survey and classification on applications of antenna in health care domain: data transmission, diagnosis and treatment," *Sādhanā*, vol. 46, no. 2, Apr. 2021, Art. no. 68, https://doi.org/10.1007/s12046-021-01586-4.

[4] Y. Feng, Z. Li, L. Qi, W. Shen, and G. Li, "A compact and miniaturized implantable antenna for ISM band in wireless cardiac pacemaker system," *Scientific Reports*, vol. 12, no. 1, Jan. 2022, Art. no. 238, https://doi.org/10.1038/s41598-021-04404-3.

[5] H. Yuliandoko, E. Setijadi, and P. Handayani, "Miniaturization Microstrip Antenna for WPT Implantable Antenna by Using Fractal and DGS Techniques," in *2023 6th International Seminar on Research of Information Technology and Intelligent Systems*, Batam, Indonesia, 2023, pp. 186–190, https://doi.org/10.1109/ISRITI60336.2023.10467950.

[6] N. A. Malik, P. Sant, T. Ajmal, and M. Ur-Rehman, "Implantable Antennas for Bio-Medical Applications," *IEEE Journal of Electromagnetics, RF and Microwaves in Medicine and Biology*, vol. 5, no. 1, pp. 84–96, Mar. 2021, https://doi.org/10.1109/JERM.2020.3026588.

[7] H. Yuliandoko, E. Setijadi, and P. Handayani, "Dual band Implantable antenna based on DGS and Sierpinski Carpets Fractal miniaturization," in *2024 IEEE Asia-Pacific Microwave Conference*, Bali, Indonesia, 2024, pp. 1126–1128, https://doi.org/10.1109/APMC60911.2024.10867600.

[8] A. Valanarasi and R. Dhanasekaran, "Optimum Band ε Shaped Miniature Implantable Antennas for Telemetry Applications," *IEEE Transactions on Antennas and Propagation*, vol. 69, no. 1, pp. 55–63, Jan. 2021, https://doi.org/10.1109/TAP.2020.3008622.

[9] R. Kangeyan and M. Karthikeyan, "Miniaturized meander-line dual-band implantable antenna for biotelemetry applications," *ETRI Journal*, vol. 46, no. 3, pp. 413–420, June 2024, https://doi.org/10.4218/etrij.2023-0050.

[10] P. Leelatien, "A Miniaturized Slotted Patch Antenna for Medical Implant Applications," in *Proceedings of the 2023 13th International Conference on Biomedical Engineering and Technology*, Tokyo, Japan, 2023, pp. 148–152, https://doi.org/10.1145/3620679.3620703.

[11] Y. E. Hachimi, E. M. Louragli, S. A. N. Arockiam, V. Subramanian, S. Das, and A. Farchi, "Design of a Miniaturized Dual-Band Antenna using Slotted Techniques for 2.45/5.8 GHz Microwave Band RFID Utilizations," *Engineering, Technology & Applied Science Research*, vol. 15, no. 1, pp. 20018–20023, Feb. 2025, https://doi.org/10.48084/etasr.9483.

[12] S. Azzaz-Rahmani, H. Zerrouki, and L. Dekkiche, "Novel Microstrip Patch Antenna for implantable medical telemetry devices," *Journal of Applied Science and Engineering*, vol. 24, no. 6, pp. 853–860, June 2021, https://doi.org/10.6180/jase.202112_24(6).0005.

[13] A. Q. Kamil, "A Dual-Band Implantable Antenna for Mobile Systems," *Engineering, Technology & Applied Science Research*, vol. 15, no. 2, pp. 20709–20713, Apr. 2025, https://doi.org/10.48084/etasr.9035.

[14] X. Hu, W. Yin, F. Du, C. Zhang, P. Xiao, and G. Li, "Biomedical applications and challenges of in-body implantable antenna for implantable medical devices: A review," *AEU - International Journal of*

Electronics and Communications, vol. 174, Jan. 2024, Art. no. 155053, https://doi.org/10.1016/j.aeue.2023.155053.

[15] E. Y. Chow, M. M. Morris, and P. P. Irazoqui, "Implantable RF Medical Devices: The Benefits of High-Speed Communication and Much Greater Communication Distances in Biomedical Applications," *IEEE Microwave Magazine*, vol. 14, no. 4, pp. 64–73, June 2013, https://doi.org/10.1109/MMM.2013.2248586.

[16] A. C. Joshi, J. C. Dash, and D. Sarkar, "Radiative Wireless Power Transfer System using Circularly Polarised Transmitter-Receiver Antenna Module to Improve Power-Transfer-Efficiency," in *2022 16th European Conference on Antennas and Propagation*, Madrid, Spain, 2022, pp. 1–5, https://doi.org/10.23919/EuCAP53622.2022.9769618.

[17] U. Krishnamoorthy, P. Lakshmipathy, M. Ramya, and H. H. Fayek, "Navigating the future of healthcare with innovations and challenges in implantable battery technology for biomedical devices," *Discover Applied Sciences*, vol. 6, no. 11, Nov. 2024, Art. no. 584, https://doi.org/10.1007/s42452-024-06278-2.

[18] M. M. Soliman *et al.*, "Review on Medical Implantable Antenna Technology and Imminent Research Challenges," *Sensors*, vol. 21, no. 9, May 2021, Art. no. 3163, https://doi.org/10.3390/s21093163.

[19] T. Kshitija, S. Ramakrishna, S. B. Shirol, and P. Kumar, "Micro - Strip Patch Antenna Using Various Types of Feeding Techniques: An Implementation," in *2019 International Conference on Intelligent Sustainable Systems*, Palladam, India, 2019, pp. 318–322, https://doi.org/10.1109/ISS1.2019.8908066.

[20] N. Kaur, N. Sharma, and N. Singh, "A Study Of Different Feeding Mechanisms In Microstrip Patch Antenna," *International Journal of Microwaves Applications*, vol. 6, no. 1, pp. 5–9, Jan. 2017.

[21] Y. Ji, L. Ge, J. Wang, and W. Wu, "Miniaturized Broadband Patch Antenna Partially Loaded With High Permittivity Dielectric," in *2020 IEEE MTT-S International Wireless Symposium*, Shanghai, China, 2020, pp. 1–3, https://doi.org/10.1109/IWS49314.2020.9360182.

[22] R. Kiruthika and T. Shanmuganantham, "Comparison of different shapes in microstrip patch antenna for X-band applications," in *2016 International Conference on Emerging Technological Trends*, Kollam, India, 2016, pp. 1–6, https://doi.org/10.1109/ICETT.2016.7873722.

[23] D. Pozar, "Input impedance and mutual coupling of rectangular microstrip antennas," *IEEE Transactions on Antennas and Propagation*, vol. 30, no. 6, pp. 1191–1196, Nov. 1982, https://doi.org/10.1109/TAP.1982.1142934.

[24] P. Kumar and G. Singh, "Microstrip Antennas Loaded with Shorting Post," *Engineering*, vol. 1, no. 1, pp. 41–45, June 2009, https://doi.org/10.4236/eng.2009.11006.

[25] R. Akhbar, H. Ja'afar, N. H. A. Rahman, N. Ramli, and R. Abdullah, "A Brief Review on Shorting Vias Techniques for Gain Enhancement in Microstrip Patch Antenna," in *2023 IEEE Symposium on Wireless Technology & Applications*, Kuala Lumpur, Malaysia, 2023, pp. 35–39, https://doi.org/10.1109/ISWTA58588.2023.10249815.

[26] A. Gupta, V. Kumar, D. K. Garg, and A. J. A. Al-Gburi, "Machine learning-based reflection coefficient and impedance prediction for a meandered slot patch antenna," *Materials Science in Semiconductor Processing*, vol. 188, Mar. 2025, Art. no. 109245, https://doi.org/10.1016/j.mssp.2024.109245.

[27] S. R. Agilesh, B. T. P. Madhav, A. Gangadhar, and S. S. Chintalapati, "Design of Dual Band Substrate Integrated Waveguide (SIW) Antenna with Modified Slot for Ka-Band Applications," *Engineering, Technology & Applied Science Research*, vol. 14, no. 4, pp. 14923–14928, Aug. 2024, https://doi.org/10.48084/etasr.7620.

[28] O. W. Ata, M. Salamin, and K. Abusabha, "Double U-slot rectangular patch antenna for multiband applications," *Computers & Electrical Engineering*, vol. 84, June 2020, Art. no. 106608, https://doi.org/10.1016/j.compeleceng.2020.106608.

[29] X. Y. Liu, Z. T. Wu, Y. Fan, and E. M. Tentzeris, "A Miniaturized CSRR Loaded Wide-Beamwidth Circularly Polarized Implantable Antenna for Subcutaneous Real-Time Glucose Monitoring," *IEEE Antennas and Wireless Propagation Letters*, vol. 16, pp. 577–580, 2017, https://doi.org/10.1109/LAWP.2016.2590477.